Multiscale multiagent architecture validation by virtual instruments in molecular dynamics experiments

Manuel Combes, Benjamin Buin, Marc Parenthoën, Jacques Tisseau

Multiscale multiagent architecture validation by virtual instruments in molecular dynamics experiments

M. Combes[a], B. Buin[a], M. Parenthoen[a], and J. Tisseau[a].

[a]LISyC, European University of Brittany(UEB)
25 rue Claude Chappe, F-29280 Plouzane, France

A multiagent architecture is proposed in order to build a physics laboratory in virtual reality. Thermodynamics experiments are used for its validation. Classical numerical resolution of thermodynamics problems comes up against the number and variability of boundary conditions. Based on molecular dynamics, a multiagent approach is proposed, resting upon agent spatial and temporal autonomy. This approach grants each particle a capacity to identify its environment using both its own clock and perceptive medium. Individual molecular properties are injected into thermal and mechanical models, and macroscopic gas behaviors can be detected and quantified by 3D virtual instruments, created in order to involve the user into the simulation. In order to assess its ability to simulate thermodynamic experiments, our method is applied to classical situations, such as the Joule-Gay Lussac experiment or the maxwellian relaxation in a hard-sphere gas. The simulated gas behavior is in good agreement with theoretical results for gases without interaction. Taking into account the volume of the molecules, our method also allows to quantify the mean free path and the average collision time for Neon and Xenon hard-sphere gases at equilibrium. Dynamic speed relaxation from uniform to maxwellian distribution is simulated successfully, and molecular covolume are also measured with such virtual gases.

1. INTRODUCTION

Thermodynamics is the branch of Physics that is concerned with the relationship between heat and other forms of energy, by coupling various mechanical interactions, such as collision, diffusion and convection. Its application to refrigerators or engines is common, but thermodynamics also examine global change and particles accelerator, implying highly multiscale phenomena. Such problems are generally modelled by partial differential equations, numerically resolved, for instance with finite volume or finite element methods [1–3].
However these methods are not efficient as regards boundary conditions variability, in particular in complex situations involving many physical interactions, with various scales of space and time [4–6]. In this case it is impossible to solve exactly even simple problems like gas behavior with pressure variations, because at macroscopic scale, any gas approximately contains 10^{23} entities.
A method has been developed for fifty years to by-pass this problem, injecting individual microscopic properties in physical models, in order to simulate macroscopic experiments. This branch of physics is called molecular dynamics [7–9], and allows to deal with complex boundary conditions. Now, the approach we propose uses various specialized entities : they are not only provided with individual properties, but also with interactions (perception, communication) between them. Particles are simulated by material agents that build their own perceptive medium, and other agents manage asynchronously the interactions between particles. That is why this approach is called multiagent simulation [10], resting upon individual-based models [11]. At different scales, other agents are used to create virtual instruments, in order to measure macroscopic physical values. In terms of method validation, the advantage of molecular dynamics is that we do know many experimental and theoretical results, which allows us to assess the relevance of such a multiagent architecture.
In this article, a simple thermodynamic system is

examined in virtual reality: a gas, whose complexity can be chosen, is submitted to various experiments with well known theoretical results. We first consider ideal gas equilibrium and expansion, and then study dynamic experiments for hard-sphere gases. This validation may allow us to apply our multiagent approach to more difficult problems, for instance dynamic energy transfer process, which is based on both mechanics and thermodynamics.

2. multiagent ARCHITECTURE

In order to study complex boundary conditions, we have built a multiagent system architecture.

2.1. Physical individual-based models

A complex system is *a priori* open, heterogeneous and formed by entities that can be complex too. In this case, the system presents different levels of structure and interaction, resting upon different scales of time and space [12]. Simulating physics in a virtual environment, created specially for this application, implies to pay attention to causality problems : physical models will only show what they were built to show [13]. In virtual reality, the model user can *a priori* interact with the simulation. This kind of work has a lot of common points with experimental sciences, but presents an access to numerical methods. We call it "*in virtuo* experiments" [14]. Hence emerging results are the product of both simulated system and user.
In individual-based models, the state is a structured set of objects described not only by variables' values, but also by fluctuating relations between entities [15]. Such a system is called multiagent system, able to carry out complex collective tasks in dynamic environments, without external control or central coordination, like insect colonies or immune systems. The autonomous character of an agent is not in its behavior, since it is restricted by determinist laws, but in its ability to observe its own dynamics and those of its neighbours. The central idea consists in providing the agents with a capacity to recognize its neighbourhood, and to interact with it in three steps : perception/decision/action.

In this study, the multiagent approach enables to follow individual trajectories, softens boundary conditions management, and authorizes the coupling of interactions, as studied in many fields : hydrological modelling [16], self-organization of multi-protein structures [17,18], chemical kinetics of blood coagulation [19], or halieutic resources dynamics [20]. The present work is aimed at assessing a multiagent architecture, able to simulate physics experiments in virtual reality, and allowing the user to interact with the virtual laboratory. Moreover, this environment was developed in order to be usable without advanced knowledge in coding ; such an architecture may be used by physicists, biologists, or ecologists.

2.2. Our multiagent architecture

Molecular dynamics simulations described here are based on an enactive architecture [21] that takes place in the ARéVi environment, developed in the European Center for Virtual Reality. In this architecture, agents (molecules or interactions) are characterized by a temporal and spatial autonomy.

Time. Temporal autonomy remains in the ability of each agent to decide on its own activities. It carries its own clock to determine its activity, contrary to classical resolution methods, based upon synchronous iterations. Our agents are scheduled by asynchronous chaotic iterations [22].

Space. Spatial autonomy remains in the way that each agent perceives its neighbourhood: it builds its own perceptive space, setting specific beacons for each measurement. A beacon is a position (x, t, dx) – location, date, spatial resolution – associated to a question. Every agent able to reply to this question will participate to give an answer, if the beacon is effectively located in its influence area. Spatial scheduling is ensured by the localization of the beacons in the influence neighbourhood of the other agents.

Some multiagent simulations also use asynchronous iterations, with a variable optimized

time step [13], but this method may involve important calculation time if too many interactions are calculated, because each time step is chosen through an error evaluation of the particle acceleration. In this context, cluster dynamics may be scheduled by a fixed time step [18]. Moreover, this approach is an adequate method to solve homogene speed and low Reynolds number problems [23], but since we study here particles' collisions, a quick interaction management is required, and neighbours' beacons detection remains more adapted.

3. GAS THERMODYNAMICS

Gas thermodynamics is a good application of a multiagent system paradigm. Indeed simple gas models, whose behavior is intuitive in classical experiments, can raise important problems of boundary conditions management. We propose here to study two gas models : an ideal gas, and a Van der Waals gas. The theoretical results about these gases are known ; and because they are quite similar to low pressure real gases, their experimental behaviors are also well described [24–26].

3.1. The simulated gas models

Both ideal and hard-sphere gas models are implemented in our *in virtuo* experiments.
Ideal gas molecules have no geometrical extent and they do not see each other (there is no electrostatic potential between them). Consequently, they only collide with the walls, and these collisions are responsable of the existence of a pressure inside. The results of the ideal gas model are derived from four strong hypotheses : 1) molecular chaos at equilibrium : the vector components of position and momentum of the particles were randomly assigned in three dimensions, 2) uniform particle spatial distribution, in the absence of an external field (neither electrostatic nor gravitational) 3) isotropic distribution of virtual molecule velocity 4) independence of velocity components.

The probability density of the ideal gas speed was deduced by [27] from these four hypotheses, and explicitly depends on particle mass m and generation temperature $T = 300\,K$ [25] :

$$P_v(v) = (\frac{m}{2\pi k_B T})^{\frac{3}{2}} 4\pi v^2 \exp \frac{-mv^2}{2k_B T} \quad (1)$$

with $k_B = 1,38.10^{-23} J.K^{-1}$ the Boltzmann constant. Root mean square speed u is calculated with Maxwell's velocity distribution. Under these conditions, for N particles confined in a volume V, pressure P and temperature T of an ideal gas explicitly depend on u :

$$T = \frac{mu^2}{3k_B} \quad (2)$$

and

$$P = \frac{Nmu^2}{3V} \quad (3)$$

Last but not least, the internal energy U is a macroscopic quantity which has a very significant role in gas behavior. It is the total energy due to the motion of the ideal gas molecules. It is directly related to temperature T, and in the case of punctual particles without interaction, equipartition theorem [28] gives the relation :

$$U = \frac{3}{2} N k_B T \quad (4)$$

Finally, at equilibrium, thermodynamic variables N, P, T, V that describe an ideal gas are related by the ideal gas state equation :

$$PV = N k_B T \quad (5)$$

The hard-sphere gas model introduces particles' volume in order to take into account molecular collisions. In this case, impacts are elastic : the interaction is considered as infinitely short, and conserves the total momentum and kinetic energy, like perfect pool balls. It is a first step to Van der Waals gas model, that would also consider short range electrostatic interactions [28,29].

3.2. Virtual measuring instruments

The objective is to measure the thermodynamics quantities P and T that define a real gas state in laboratory experiments. A virtual physics laboratory was built with computing tools of the AReVi environment, developed in the European Center for Virtual Reality, in order to simulate *in*

virtuo experiments [22]. These tools permitted to create particle generators, pressure and temperature sensors, collision counters, virtual enclosures and cameras that provide an immersive video of the experiment. This virtual environment can also be provided with portals between various boxes, or obstacles like porous tubes. Gas behavior measurement permits the evaluation of instrumentation performances, in comparison with theoretical results. Equation (4) gives an *in virtuo* gas temperature definition, that is calculated by measuring in real time the kinetic energy of the system : a volume thermometer was built with a cube that works like a counter, adding kinetic energies of all the particles present in its volume at time t.

$$T_{thermo} = \frac{U_{thermo}}{\frac{3}{2}.N_{thermo}.k_B} = \frac{\sum_{i=1}^{N_{thermo}} \frac{1}{2} m_i v_i^2}{\frac{3}{2}.N_{thermo}.k_B} \quad (6)$$

We choose to calculate the average temperature, with X measurements. For that reason, we do not measure exactly the root mean square speed, and it would be the case only with a statistical number (almost 10^{23}) of particles in the volume. This point will be discussed later on.
Pressure sensors (manometers) also realize statistical measurement. An infinitely thin disk counts during a time t_{mano} the number of particles that bounce on its surface S. Then each manometer adds the momentum variation $\Delta\vec{p} = m\Delta\vec{v}$ of all these particles, and taking into account the particles' angle of incidence, pressure is defined by :

$$P_{mano} = \frac{2}{t_{mano}.S} \sum_{i=1}^{N_{mano}} m_i.v_i.cos(\vec{v_i}; \vec{n}) \quad (7)$$

for one direction. Since two manometers oriented in two directions would present two distinct pressure values, a three-dimensional solution is proposed : using three orthogonal surfaces, each particle projetcs its total contribution on an orthonormal basis (X, Y, Z), and the average value in calculated. It should be noticed that pressure is measured by a surface sensor, adding quantities proportional to speed, whereas temperature is evaluated by a volume, adding quantities proportional to speed squared. Nevertheless, pressure and temperature are supposed to be proportionnal. Actually, this apparent paradox is justified because temperature is defined as a statistical instantaneous mean, whereas pressure is a temporal mean. Indeed, dividing by elementary time dt permits sensors to take into account the particle collision frequency, so that the fastest particles have a large influence on temperature, because they bounce on the manometer more often. That is why *in virtuo* pressure is coherent with the corresponding temperature, and both respect the ideal gas law.

4. *IN VIRTUO* EXPERIMENTS

4.1. Ideal gas law

Macroscopic pressure and temperature are measured in a virtual $10\,nm$ side enclosure, containing 8000 Xenon particles of molar mass $M = 131,29.10^{-3}\,g.mol^{-1}$. The particle generator ensures a maxwellian velocity distribution, with a generation temperature $T = 300\,K$. The principle of inertia rules each particle's dynamics between two successive bounces. Collisions are supposed to be elastic, *i.e.* the total kinetic energy remains constant, and consequently the molecule speed too. The agent-molecule verifies at each step (time t) that it still remains inside the box. If it does, it keeps on its way ; if it does not, it is reinjected at next step (time $t + dt$) as if it was a symmetric bounce. The virtual instruments used for this experiment are similar to the sensors presented on figure 1.

The simulated gas is in thermodynamic equilibrium within the enclosure, and sensor response time is chosen as $\Delta t_{sensor} = 1.10^{-10}\,s$. The thermodynamic quantities measured are :

$$P.V = 3,301.10^{-17} \pm 0,02.10^{-17}\,J$$

$$N.k_B.T = 3,300.10^{-17}\,J$$

Temperature is determinist because the enclosure and the thermometer have the same volume, whereas pressure measurement is a temporal integration, with its associated uncertainty. It should be noticed that there is no need of 10^{23} particules to obtain a good agreement of the ideal gas law.

4.2. Joule-Gay Lussac experiment

The Joule-Gay Lussac experiment is a classical thermodynamic problem that consists in abruptly expanding a gas, initially described by To, Po, Vo, into a greater volume. A portal is instantaneously opened, without energy contribution, and the process is adiabatic (no heat transfer through the walls). Figure 1 represents the gas expansion during the virtual experiment. This expansion is theoretically isoenergetic, *i.e.* gas internal energy remains constant. In the particular case

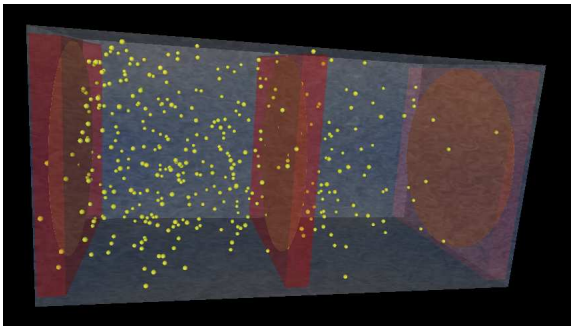

Figure 1. Joule - Gay Lussac expansion. The volume was enlarged abruptly : the gas expands in the space in an isoenergetic way. Surface manometers are brown, and volume thermometers are red.

of the perfect gas, the final temperature is equal to the initial temperature (monothermal expansion). In order to evaluate the temporal autonomy of AReVi agents, the temperature evolution is measured in real time (figure 2). Two results should be noticed here. Firstly, the Joule-Gay Lussac *in virtuo* experiment is indeed monothermal for a virtual gas without interaction. Then, during a transitory period, a thermal peak is observed. This phenomenon is also observed experimentally in laboratory and can be explained by a kinetic argument. During an expansion into an evacuated enclosure, the fastest (and thus most energetic) particles are the first to pass through the manometer surface, consequently the mea-

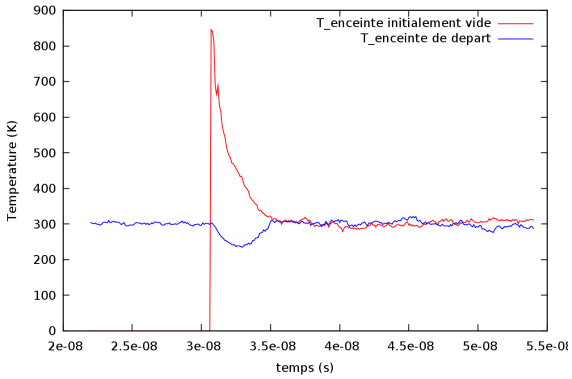

Figure 2. Temperature evolution during Joule-Gay Lussac expansion. Joule-Gay Lussac expansion is isoenergetic. For an ideal gas, the experiment is monothermal. Thermal peak is a kinetic effect. The short thermal drop in the first box illustrates gas energy conservation.

sured temperature is higher during a short transitory period. Moreover, this temperature is calculated in the laboratory referential, which gives an additional contribution to the peak, because in this case, expanded gas presents a group motion. The short thermal drop detected by the first thermometer illustrates the conservation of the total kinetic energy, since the fastest molecules were liberated first. This result highlights the efficiency of agents' temporal autonomy, since dynamic behavior can be simulated with such a multiagent architecture.

4.3. Hard-sphere gases

In order to get closer to the behavior of real gases, when pressure is not low enough to consider that molecules are blind, new microscopic characteristics can be introduced. Here, Van der Waals' hard-sphere interaction consists in simulating one to one, every elastic collision between a molecule of radius R and its neighbours.
Each agent has one main activity : to move and check if neighbours are present in its perception zone : a sphere of radius $2.v.dt + R$ surrounding each agent. For each detected neighbour, inter-

molecular distance is calculated for every step. A condition of collision is that intermolecular distance is decreasing. If this distance does not decrease, there is no collision. If it decreases, a minimum impact time is determined, and when this time is reached, the molecules do collide (elastic impact). Then, new molecular positions and velocities are calculated.
We now consider nonpunctual particles, and three experiments are carried out with Xenon and Neon hard-sphere gases.

4.3.1. Maxwellian relaxation

A dynamic experiment is implemented in order to assess the architecture ability to simulate physics out of equilibrium. A Xenon hard-sphere gas is placed in an enclosure in unstable state : the initial velocity distribution is uniform at $v_o = 238,74\, m.s^{-1}$, which corresponds to $T = 300\, K$. After $4,2.10^{-8}\, s$ of simulation, a new velocity distribution is reached, which is illustrated in figure 3. This result is in good agreement with the theoretical maxwellian relaxation

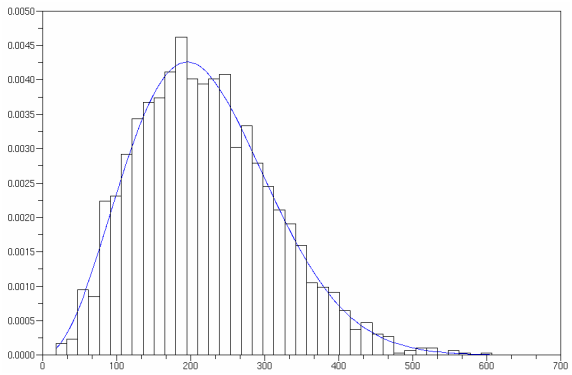

Figure 3. Speed distribution of a Xenon hard-sphere gas after $4,2.10^{-8}\, s$ of simulation. The initial speed state was uniform at $v_o = 238,74\, m.s^{-1}$. The distribution reached after relaxation is in good agreement with the theoretical curve of maxwellian distribution for $T = 300\, K$.

[25,30], which is due to elastic collisions : both total momentum and kinetic energy are conserved during a collision, and each impact contributes to energy redistribution, until the gas system reach thermodynamic equilibrium.

4.3.2. Mean free paths

An enclosure of volume V contains $N = 1000$ hard-sphere particles of radius R, with a maxwellian velocity distribution calculated with a generation temperature $T = 300\, K$. An identical box of side $L = 10\, nm$ contains a perfect gas at the same temperature. The mean free path l is defined as the average distance covered by a particle between two successive impacts. An ideal gas can be described by a mean free path l_w^{theo} for collisions on walls, and a hard-sphere gas by l_m^{theo} for collisions between molecules. Theoretical expressions of these statistical quantities can be calculated (cf Appendix A) :

$$l_w^{theo} = 0,669 * L \tag{8}$$

$$l_m^{theo} = \frac{V}{\sqrt{2}.N.4\pi R^2} \tag{9}$$

The corresponding mean collision times τ_w and τ_m are theoretically related to the mean free paths by the mean speed V_m of the distribution [25,28]:

$$l = V_m.\tau \tag{10}$$

An additional virtual instrument was created in order to measure these statistical path quantities and was called *balistometer*. At each impact with a wall or another molecule, every agent sends the balistometer both its own position and virtual date. The balistometer thus calculates the mean free path, the average collision time and the number of collisions (on the walls or between molecules) describing the experiment.
During an experiment duration t_{exp} with N particles, the sum of virtual times of every agent is equal to $N.t_{exp}$, and this quantity can also be calculated using average collision times :

$$N.t_{exp} = N_w.\tau_w = N_m.\tau_m \tag{11}$$

with N_w and N_m the numbers of impacts with a wall and a neighbor respectively, considering that N_m is double the number of molecular collisions,

since the balistometer counts every agent message. Experimental and theoretical results are listed in Table 1 for Neon and Xenon hard-sphere gases. Mean free path uncertainties are calculated with the Student-Fisher law [31]. Atom's radius R and molar mass M are given in [29].

Table 1
Experimental and theoretical statistics of Ne and Xe hard-sphere gases.

Molecule	Neon	Xenon
M $(g.mol^{-1})$	20.18	131.3
R $(10^{-10}m)$	1.54	2.16
V_m $(m.s^{-1})$	570,9	217,1
l_w^{theo} (nm)	6,691	6,691
l_w (nm)	6,689	6,688
Δl_w (nm)	0,004	0,004
l_m^{theo} (nm)	2,16	1,06
l_m (nm)	3,15	1,50
Δl_m (nm)	0,05	0,05
$V_m * \tau_m$ (nm)	3,16	1,51
$N * t_{exp}$ $(10^{-5}\,s)$	3,50	3,50
$N_w * \tau_w$ $(10^{-5}\,s)$	3,49	3,49
$N_m * \tau_m$ $(10^{-5}\,s)$	3,50	3,50

We can observe that for ideal gases, the experimental mean free path is in excellent agreement with the theoretical value, which validates the bounces management on the walls. This experiment highlights the approximation made in [25] for the theoretical calculation of l_w, which is not trivial (Appendix A). For the two hard-sphere gases, there is agreement between the experimental terms of equation (11). Nevertheless, the experimental mean free path l_m and the average collision time τ_m only correspond to the correct order of magnitude. This observation illustrates the fact that the balistometer does not count enough molecular collisions during t_{exp}. The reason could be that agents face a problem of real time adaptation of their detection zone.

4.3.3. Hard-sphere covolume

The same experimental context is used in order to evaluate the excluded covolume $N.b$ of hard-sphere gases, inaccessible for the N particules because of collisions. The initial velocity distribution of the molecules is identical in both enclosures, so temperature remains the same, but pressure effects can be observed independently. In this way, state equations can be written :

$$N.k_B.T = P_{ideal}.V = P_{collision}.(V - N.b) \qquad (12)$$

which suggests two methods to measure molecular covolume b : one direct, calculating (T, P) in the Van der Waals enclosure, and using the state equation ; and one indirect, comparing the pressure values in the two boxes :

$$b_{direct} = \frac{V}{N} - \frac{k_B.T}{P_{collision}} \qquad (13)$$

$$b_{indirect} = \frac{V}{N}.(1 - \frac{P_{ideal}}{P_{collision}}) \qquad (14)$$

In the hard-sphere gas model, when two spheres A and B are in contact, the excluded volume for one molecule is half the volume of a shpere of radius $R_A + R_B$:

$$V = (\frac{4}{3}\pi(R_A + R_B)^3)\frac{1}{2} = 4.(\frac{4}{3}\pi R^3) \qquad (15)$$

This molecular covolume is slightly different of the usual experimental results because the Van der Waals' radius is used here, which is a little bigger than the minimum approach distance, since it is defined as the distance between non-linked atoms in crystals.

For this experiment, Neon and Xenon characteristics and measurements are listed in Table 2, and uncertainty Δb is calculated by error propagation. Virtual gas covolume measurements remain in a good range of values, which is interesting in terms of validation of agent spatial autonomy, but measurement uncertainties are very high relatively to covolume values.

These results are not a good agreement with the hard-sphere gas value, but they correspond quite well with experimental covolume, measured in laboratory by critical pressure measurements. This observation may question the validity of

Table 2
Direct and indirect results of covolume measurement. Uncertainty Δb is calculated by error propagation.

Molecule	Neon	Xenon
M $(g.mol^{-1})$	20.18	131.3
R $(10^{-10}m)$	1.54	2.16
b_{h-s} $(10^{-29}m^3)$	6.12	16,9
b_{direct} $(10^{-29}m^3)$	3,62	9,30
Δb_{direct} $(10^{-29}m^3)$	1,79	1,52
$b_{indirect}$ $(10^{-29}m^3)$	3,67	9,32
$\Delta b_{indirect}$ $(10^{-29}m^3)$	2,80	2,85
b_{exp} $(10^{-29}m^3)$	2,84	8,47

classical hard-sphere covolume calculation in further work.
Van der Waals' attractive coefficient may also be measured *in virtuo*, introducing molecular electric field, but the manometer needs to be more precise, because it realizes surface measurements. In order to improve the instruments' precision, a cluster management could be employed : each cluster of particles may contain a great number of molecules, and multiagent experiments would use these clusters as agents. The challenge is to manage cluster stability (in terms of velocity and position), and post-collision organization.

5. CONCLUSION

Classical thermodynamics experiments were carried out in virtual reality, using a multiagent approach. This method, resting upon individual-based systems, consists in injecting microscopic data into gas models, and measuring macroscopic quantities thanks to virtual instruments. The multiagent architecture used in this work grants each agent a temporal and spatial autonomy, which permits us to simulate various macroscopic phenomena in a virtual physics laboratory. Our simulated ideal gas corresponds very well to its theoretical macroscopic state law. Moreover, isoenergetic behavior was accurately observed during the Joule-Gay Lussac experiment, with its characteristic kinetic thermal peak. This experiment assesses the efficiency of agents temporal autonomy. In addition, Neon and Xenon hard-sphere gases were simulated in order to validate agents spatial autonomy. Mean free paths and average collision times were measured in good agreement with theoretical previsions, concerning collision on walls. Nevertheless, improvements are necessary concerning real time adaptation of the detection zone around the agents, in order to measure precise mean free paths between molecules. Molecular covolume of Neon and Xenon measured *in virtuo* are of the order of magnitude of usual geometrical and experimental values, but measurement resolution must be improved. In order to do so, a better manometer precison is required, and many more molecules should be simulated, working on the link between individual and population, by managing clusters of particles. During this study, virtual instruments were validated and may now be applied by any user to more difficult thermodynamic problems. A future application is the dynamic heat transfer in gases, operated for instance by pressure force work on interacting molecules, during the expansion of a hard-sphere gas into an empty enclosure. The present multiagent architecture may also simulate more complex systems. A multi-interaction application may be implemented with heat transfer, viscous forces and pressure forces that occur during the ascent of buoyant bodies in magmatic flows [32]. Few multiagent approaches have been carried out for volcanic phenomena [33], and although its multiagent architecture is relevant, its physical mechanisms are not demonstrated. We now aim at implementing reliable geophysical models in virtual reality.

APPENDIX A : Mean free paths

Between two molecular impacts

After each impact, the relative velocity $\vec{V_{rel}}$ between a molecule A and its next target B is randomly distributed. In this direction, during Δt, the molecule A will make $< N_c >$ collisions on an average. $< N_c >$ is defined as the number of particles present in a tube of axis $\vec{V_{rel}}$, of radius

$R_A + R_B$ and of length $< \vec{V_{rel}} > .\Delta t$ [34] :

$$< N_c >= \pi(R_A + R_B)^2 . < \vec{V_{rel}} > .\Delta t.\rho \qquad (16)$$

with $\rho = \frac{N}{V}$ the gas density in the enclosure. The quantity $\sigma = \pi(R_A + R_B)^2$ is the collision cross-section of the hard-sphere gas [35]. The average collision time τ_m for molecular impacts is defined by the time Δt corresponding to $< N_c >= 1$:

$$\tau_c = \frac{1}{< V_{rel} > .\sigma.\rho} \qquad (17)$$

The average quantity $< V_{rel} >$ can be calculated in the center of mass reference frame. It can be demonstrated [28,30] that a virtual particle of mass $\mu = \frac{m_A.m_B}{m_A+m_B} = \frac{m}{2}$ and of velocity $\vec{V_{rel}}$ is distributed with the Maxwell's distribution law. Thus for an ideal gas at temperature T, the average relative velocity is :

$$< V_{rel} >= \sqrt{\frac{8k_BT}{\pi\mu}} = \sqrt{2}.V_m \qquad (18)$$

and using equation (10), the theoretical expression of the mean free path between two successive molecular impacts is :

$$l_m^{theo} = \frac{V}{\sqrt{2}.N.4\pi R^2} \qquad (19)$$

Between two wall impacts

The elastic collisions properties allow us to calculate the average distance between two successive impacts with an infinite pile of 3D boxes of side L. Thus the mean free path is the average distance between two walls. For a particule from (0,0,0) to (x,y,z), the distance is $r = \sqrt{x^2+y^2+z^2}$ and the number of walls encountered is $\frac{x+y+z}{L}$. Then the average value of $\frac{L.\sqrt{x^2+y^2+z^2}}{x+y+z}$ is calculated in spherical coordinates, with equiprobable directions on $\frac{1}{8}$ of the 3D space, since x, y and z are considered as positive values. The corresponding integral is not trivial, and can be calculated numerically :

$$l_w^{theo} = \frac{4.L}{\pi} \int_1^{\sqrt{2}} \frac{\frac{\pi}{2}u - ln(u)}{(1+u^2)\sqrt{2-u^2}} du = 0,6691.L$$

ACKNOWLEDGMENTS

The authors particularly thank Frédéric Massias, Pascal Redou and Laurent Gaubert for their highly constructive remarks about thermodynamics and statistics. Nasser Soilihi and Cyril Delbègue, from the National Engineering School of Brest (ENIB), contributed very significantly to the coding of thermodynamic simulations.

REFERENCES

1. M. Matsui, G. D. Price, and A. Patel, *Comparison between the lattice dynamics and molecular dynamics methods: Calculation results for MgSiO3 perovskite*, Geophys. Res. Lett., 21(15), 1659-1662, 1994.
2. E. Bansch, F. Hausser, and A. Voigt, *Finite Element Method for Epitaxial Growth with Thermodynamic Boundary Conditions*, SIAM journal on scientific computing, vol. 26, no6, pp. 2029-2046, 2005.
3. L. Yuan and L. Kaitai, *Penalty finite element method for Stokes problem with nonlinear slip boundary conditions*, Applied mathematics and computation, 204, 216-226, 2008.
4. H. Houde, H. Changhong and W. Xiaonan, *Analysis of artificial boundary conditions for exterior boundary value problems in three dimensions*, Numerische Mathematik, vol. 85, no3, pp. 367-386, 2000.
5. M. Takeda, M. Zhang and N. Takeno, *Quantitative Evaluation of the Effects of Hydrogeological Boundary and Initial Conditions on Slug Tests*, Practice Periodical of Hazardous, Toxic and Radioactive Waste Management, 11(1), 2007.
6. P. Redou, G. Desmeulles, J-F. Abgrall, V. Rodin and J. Tisseau, *Formal validation of asynchronous interaction-agents algorithms for reaction-diffusion problems*, 21st International Workshop on Principles of Advanced and Distributed Simulation, USA, 2007.
7. B.J. Alder and T.E. Wainwright, *Studies in molecular dynamics. I. General Method*, Journal of Chemical Physics, 1959.
8. M.P. Allen and D.J. Tideslay, *Computer simulation of liquids*, Clarendon Press, 1989.

9. D. Frenkel and B. Smit, *Understanding Molecular Simulation: From Algorithms to Applications*, Academic Press Inc, 2001.
10. G. Weiss, *Multiagent Systems: A Modern Approach to Distributed Artificial Intelligence* , MIT Press Cambridge, 1999.
11. V. Grimm, U. Berger, F. Bastiansen, S. Eliassen, V. Ginot, J. Giske, J. Goss-Custard, T. Grand, S.K. Heinz, G. Huse, A. Huth, J.U. Jepsen, C. Jorgensen, W.M. Mooij, B. Muller, G. Pe'er, C. Piou, S.F. Railsback, A.M. Robbins, M.M. Robbins, E. Rossmanith, N. Ruger, E. Strand, S. Souissi, R.A. Stillman, R. Vabo, U. Visser and D.L. DeAngelis, *A standard protocol for describing individual-based and agent-based models*, Ecological modelling, 198, 115-126, 2006.
12. J. Tisseau, *Realite virtuelle et complexite. Expérimentation* in virtuo *des systèmes complexes*, Manifeste scientifique du Centre Europeen de Realite Virtuelle, France, 2004.
13. A. Coulon, *Modelisation cellulaire pour l'emergence de structures multiproteiques auto-organisees*, Technique et science informatiques, RSTI serie TSI, Vol. 26 N 1-2, 2007.
14. J. Tisseau, *Realite virtuelle : autonomie in virtuo*, Habilitation Diriger des Recherches, Universite de Rennes 1, 2001.
15. F. Bousquet, C. Le Page and J-P. Mller, *Modelisation et simulations multiagents*, Actes des deuximes assises nationales du GDR I3, pp. 173-182, Nancy, France, 2002.
16. D. Servat, *Modelisation de dynamiques de flux par agents. Application aux processus de ruissellement, infiltration et erosion*, thse de doctorat, Universite de Paris 6, France, 2000.
17. H. Soula, C. Robardet, F. Perrin, S. Grippon, G. Beslon and O. Gandrillon, *modelling the emergence of multi-protein dynamic structures by principles of self-organization through the use of 3DSpi, a multiagent-based software*, BMC Bioinformatics, 6:228, 2005.
18. A. Coulon, G. Beslon and O. Gandrillon, *Large Multiprotein Structures modelling and Simulation: The Need for Mesoscopic Models*, Methods in Molecular Biology, 484, 2008.
19. S. Kerdelo, *Methodes informatiques pour l'experimentation in virtuo de la cinetique biochimique. Application la coagulation du sang*, thse de doctorat, Universite de Bretagne Occidentale, Brest, France, 2006.
20. S. Bonneaud, P. Redou and P. Chevaillier, *Pattern oriented agent-based multimodelling of exploited ecosystems*, 6th EUROSIM congress, Slovenia, 2007.
21. M. Parenthon and J. Tisseau, *Tutorial book of virtual concept. Enactive modelling*, ENSIAME/LIPSI-ESTIA, France, 2005.
22. F. Harrouet, E. Cazeaux and T. Jourdan, *Le traite de la Realite Virtuelle. AReVi*,Presses de l'Ecole des Mines, pp. 369-392, 2006.
23. E. Guyon, J-P. Hulin and L. Petit, *Hydrodynamique physique*, CNRS Editions, 2001.
24. S. Colgate, C. Sona, K. Reed and A. Sivaraman, *Experimental ideal gas reference state heat capacities of gases and vapors*, Journal of chemical and engineering data, 35, 1, 1990.
25. J-P. Pérez, *Thermodynamique. Fondements et applications*, 3e edition, Dunod, 2001.
26. I. Trifonov, *Experimental verification of Boyle's law and the ideal gas law*, Physics education, vol. 42, no2, pp. 193-197, 2007.
27. J.C. Maxwell, *On the dynamical Theory of Gases*, read May 31, 1866 ; Philosophical Transactions of the Royal Society of London, vol. 157, pp. 49-88, 1867.
28. G. Bruhat, *Cours de Physique Generale - Thermodynamique*, Masson, 6^e ed., 1968.
29. A. Gerschel, *Liaisons intermoleculaires*, InterEditions / CNRS Editions, 1995.
30. L. Landau and E. Lifchitz, *Physique theorique. Physique statistique*, 4^e edition, MIR Moscou, Ellipses, 1994.
31. R. A. Fisher, *Applications of "Student"'s distribution*, Metron, 5: 90-104, 1925.
32. E. Burov, C. Jaupart and L. Guillou-Frottier, *Ascent and emplacement of buoyant magma bodies in brittle-ductile upper crust*, Journal of Geophysical Research, 108, B4, 2003.
33. P. Marcenac, *Modélisation de systmes complexes par agent*, Technique et science informatiques, vol 16 - no 8, 1013-1037, 1997.
34. J-P. Pérez, *Mécanique. Fondements et applications*, 6e edition, Dunod, 2001.
35. R.G. Newton, *Scattering theory of waves and particles*, McGraw Hill, 1966.